Applied Catalysis B: Environmental 182 (2016) 132–141

Contents lists available at ScienceDirect

Applied Catalysis B: Environmental

journal homepage: www.elsevier.com/locate/apcatb

Degradation of pharmaceuticals in wastewater using immobilized TiO_2 photocatalysis under simulated solar irradiation

Yujie He*, Nora B. Sutton, Huub H.H. Rijnaarts, Alette A.M. Langenhoff

Department of Environmental Technology, Wageningen University, P.O. Box 17, 6700 EV Wageningen, The Netherlands

ARTICLE INFO

Article history:
Received 16 June 2015
Received in revised form 14 August 2015
Accepted 5 September 2015
Available online 9 September 2015

Keywords:
Pharmaceuticals
Photocatalysis
Sunlight
DOM
Application

ABSTRACT

Pharmaceutically active compounds (PhACs) are not efficiently removed in wastewater treatment plants and are released into surface waters resulting in toxin accumulation. The aims of this study were to investigate the effect of solar irradiation on PhACs in wastewater using immobilized TiO_2 present as a catalyst, and to study the potential of this photocatalysis technique as a post-treatment process for wastewater effluent. We treated a mixture of PhACs spiked in wastewater effluent and in deionized water as a control with simulated solar irradiation for 96 h. Experiments were conducted with immobilized TiO_2 (photocatalysis) and without (photolysis). First, TiO_2 was successfully immobilized on 200–500 μm sand by using a sol–gel method. The photocatalysis resulted in high removal efficiencies for poorly biodegradable PhACs in wastewater effluent: 100% for propranolol, 100% for diclofenac, and 76 ± 3% for carbamazepine. Photodegradation of all four PhACs followed pseudo-first-order kinetics, and the kinetic constant of photocatalysis was much higher than that of photolysis in the absence of a catalyst. Dissolved organic matter (DOM) in wastewater effluent enhanced photodegradation of PhACs by producing reactive radicals. However, at the same time, DOM inhibited photodegradation, possibly because DOM reforms the oxidation intermediates of PhACs into parent compounds. From an application perspective, water depth was confirmed as a key factor in photodegradation of PhACs due to light attenuation by modelling and experimental results. In addition, after photocatalysis, toxicity of PhACs decreased and biodegradability of wastewater effluent increased slightly. In conclusion, the technique is a promising post-treatment process to improve water quality, prior to discharging to natural waters or to polishing water treatment systems such as wetlands and lagoons.

1. Introduction

Many pharmaceutically active compounds (PhACs) behave as persistent organic micropollutants, as evidenced by their continuous input and accumulation in the environment [1]. PhACs are released into the aquatic environment, primarily due to their incomplete removal by conventional treatment processes in wastewater treatment plants (WWTPs) [2]. PhACs are evidenced or suspected to provoke toxic effects on living organisms even when present at concentrations as low as ng/l level [3]. Consequently, the accumulation of PhACs poses a threat to the quality of water resources. Advanced technologies such as application of UV and ozonation are effective for treating some PhACs, but have limited applicability due to high construction, maintenance and energy costs [4]. Therefore, more efficient treatment techniques need to be explored and further developed to eliminate PhACs emissions to the environment.

Multiple biotic and abiotic routes could transform PhACs once they reach the surface water [5]. One of the abiotic processes is photodegradation, which is a significant and predominant pathway to remove PhACs in natural water treatment systems such as wetlands, ponds and lagoons [6]. In addition, photodegradation has been considered as an effective remediation tool for wastewater, especially for increasing the biodegradability of contaminants and detoxifying the effluent stream [7]. In order to maximize photodegradation performance, photocatalysis has often been combined with solar irradiation, which could provide a more economically feasible and ecologically effective alternative, as compared to using artificial light sources. Photolysis and photocatalysis of PhACs have been investigated previously, mostly in pure water or surface water matrices under UV irradiation [8–11]. However, to our knowledge, PhACs removal by both photolysis and photocata-

* Corresponding author. Fax: +31 0 317 482108.
E-mail addresses: yujie.he@wur.nl (Y. He), nora.sutton@wur.nl (N.B. Sutton), huub.rijnaarts@wur.nl (H.H.H. Rijnaarts), alette.langenhoff@wur.nl (A.A.M. Langenhoff).

http://dx.doi.org/10.1016/j.apcatb.2015.09.015
0926-3373/

lysis from wastewater effluent (WWE) under solar irradiation has only been studied by a few groups [12,13].

In our study, we focused on PhACs that are most commonly detected in wastewater affected water systems and aquatic organisms [14,15], and are not easily biodegradable: propranolol (PRO, β-blocker), carbamazepine (CBZ, antiepileptics), ibuprofen and diclofenac (IBP and DFC, anti-inflammatories and analgesics). For example, removal efficiencies of CBZ and DFC in WWTPs have been reported below 30% and 21–40% respectively [16]. TiO_2 has been most extensively used in photocatalytic reactions because it is biologically and chemically inert, inexpensive, and non-toxic [17]. In addition, at sea-level heights of the surface of the Earth, the sun could still provide sufficient light intensity and available spectrum to activate TiO_2 [18]. However, TiO_2 nanoparticles may exert ecotoxicological effects on aquatic microorganisms. For example, the half maximal effective concentration (EC50) of TiO_2 (25 nm) was determined about 40 mg/l for algae [19]. According to the EU Directive on classification, packaging and labelling of dangerous substances [20], a toxicity in the range of 10–100 mg/l is classified as harmful to aquatic organisms; and may cause long-term adverse effects in the aquatic environment. Thus a non-dispersed method is needed when applying TiO_2 in open water treatment systems. To this end, we immobilized TiO_2 on sand to avoid this potential of aquatic system pollution. Previously, Avisar et al. [21] reported a 35% reduction of CBZ in surface water and negligible removal in WWE, when the matrices exposed to solar irradiation simulated by a 150 W Xenon arc lamp in the presence of nitrogen-doped TiO_2-coated glass slides.

In this study, we aim to evaluate the application of photocatalysis for PhACs removal in WWE by combing solar light and immobilized TiO_2. To determine the feasibility of such a system, and for proper design of experiments, we analyzed the light attenuation at various water depths and its effect on photolysis efficiency of PhACs mathematically and experimentally. Based on the optimized depth, we investigated the reaction mechanisms of target PhACs spiked in WWE under simulated solar irradiation. Additionally, in order to test the potential application of the photocatalysis, we analyzed the change of PhACs in toxicity and biodegradability during photodegradation. The outcome of this work contributes to understanding the solar induced photocatalysis as a low-cost, efficient treatment technique to remove PhACs as a post-WWTP process, before WWE is discharged into surface waters, such as lakes, rivers, natural wetlands, ponds, and lagoons.

2. Materials and methods

2.1. Chemicals

Chemicals were purchased from Sigma–Aldrich (USA) at various purity grades: (±)-propranolol hydrochloride (≥99%), diclofenac sodium salt (≥99%), carbamazepine (≥99%), and ibuprofen (≥98%). Table A.1 shows the physical and chemical characteristics of target PhACs. Fenoprofen calcium salt (≥97%) and hydrate 10, 11-dihydrocarbamazepine (≥99%) were used as internal standards (Sigma–Aldrich, USA). Acetonitrile with 0.1% formic acid, water with 0.1% formic acid, and methanol (Biosolve B.V., The Netherlands) were used for ultra-performance liquid chromatography (UPLC) analysis. Titanium (IV) butoxide (≥97%, Sigma–Aldrich), HNO_3 (Merck, Germany), ethanol (≥99%, Merck) and glacial acetic acid (100%, Merck) were used to immobilize the catalyst. All the other reagents used were of analytical grade or higher. Deionized water (DI) from a Milli-Q system (Millipore, Bedford, MA, USA) was used to prepare all solutions. All glassware was manually cleaned with detergent, acetone, DI, and air-dried before using.

2.2. Immobilization techniques

The purchased quartz sand (Happy home, The Netherlands) was already pre-rinsed by acid. The sand was sieved to obtain 200–500 μm fractions, mixed with DI, stirred for 24 h, and air-dried prior to being used as the immobilization substrate. TiO_2 was coated on the sand by using the sol–gel method based on the work of Xia et al. [22]. Firstly, 14.2 ml of Titanium (IV) butoxide was added to 50 ml of ethanol and then the mixture was stirred continuously with a magnetic bar at 300 rpm for 10 min (Heidolph MR 3001K, Germany). In this step, white precipitation should be avoided, otherwise the gel would not be formed. Secondly, 1 ml of 0.1 mol/l HNO_3, 1 ml of DI and 1 ml of glacial acetic acid were sequentially added drop-wise. After stirring for 6–7 min at 300 rpm at room temperature, a pale-yellow gel was formed. Next, 25 g sand, as the substrate for immobilization, was poured slowly into the gel and stirred for 15 min at 350 rpm. Finally, the gel mixture was dried for 2 h at 105 °C in the oven (Heraeus Hanau, Germany). After totally cooling down in the oven, the 1-layer immobilized material was calcined for 3 h at 500 °C and then cooled in the oven. The temperature of the oven was raised and cooled slowly before and after calcination to avoid cracking of the wrapped gel. The coating process was repeated twice more on the 1-layer immobilized sand to get 3-layers of immobilized material.

2.3. Photodegradation experiments

In order to simulate solar light, Xenon high-intensity discharge lamps (55 W) with charger and battery were installed in a climate chamber (Heraeus Vötsch, Germany), in which the temperature was maintained at 25 ± 2 °C. Xe-lamps were fixed above the water surface and directly irradiated solutions. The lamps emitted irradiation in the wavelength range of 300–800 nm and the irradiation intensity at the water surface was maintained at 159 lux, which is comparable with the solar light intensity in the Netherlands (latitude 51°59′4″N, longitude 5°39′31″E, Fig. A1) Light spectrum and intensity were detected by using a USB2000+ spectrometer (Ocean optics, UK).

In order to investigate the effect of light attenuation on the photodegradation of PhACs, a 0.5 m water filled column experiment was performed by adding 5 mg/l of each PhAC in DI and irradiating for 96 h. The solution in the column was under static condition, and thus unhomogenized. Sampling points were evenly distributed on the side profile of the column so that water samples could be collected at every 0.1 m between depths of 0.0–0.5 m. Prior to the start of the experiment, needles were affixed at each sampling point. Samples were collected by attaching a syringe to each needle and slowly withdrawing liquid, thus minimizing disruption of the water column during sampling. Samples were collected every 24 h.

For the kinetic experiment, the initial concentration of individual PhACs was 5 mg/l spiked in 500 ml DI or WWE, collected from Bennekom WWTP, The Netherlands. The basic water quality data of used WWE are shown in Table A.2. WWE was filtrated by 0.45 μm filter prior to being used in experiments. Photolysis experiments were performed by only applying irradiation, while photocatalysis experiments included 25 g immobilized TiO_2. During the 96 h photodegradation, a shaking speed of 75 rpm was kept so that the solution could be homogeneous while the catalyst was still stable at the bottom of the beaker. Adsorption experiments were performed in parallel in the dark by shielding light with foil and a sealed box. For all the experiments, the solution was shaken for 1 h to be totally homogeneous in darkness, prior to withdrawing the first sample as the initial concentration C_0. WWE samples were centrifuged (IEC microlite centrifuge, Thermo, USA) at 10000 rmp for 10 min before UPLC analysis. All the experiments were performed in duplicate.

2.4. Analytical procedures

2.4.1. Basic chemical analysis

Biodegradability was evaluated using the ratio between 5-day biochemical oxygen demand (BOD_5) and chemical oxygen demand (COD). BOD_5 was determined by the OxiTop® system (WTW Weilheim, Germany) thermostated at 20 °C. COD was measured using Dr. Lange test kits (Hach Lange GmbH, Germany) on a Hach DR/3900 spectrophotometer. The dissolved organic carbon and anion of WWE was measured using a Shimadzu analyser (Japan) and ion chromatography (Dionex ICS 2100, USA). WWE samples were freeze-dried into solid material by an alpha 2-4 LD^+ freeze dryer (Martin Christ GmbH, Germany). FTIR analysis of 1 mg WWE solid was performed using a Bruker Tensor 27 FTIR spectrometer equipped with a Platinum ATR accessory (Bruker, Germany).

2.4.2. Characterization of immobilization material

Surface morphologies of raw sand and TiO_2 coated sand were analyzed by a field emission scanning electron microscope (SEM, Magellan 400, FEI, The Netherlands) with secondary electron detection at 2 kV, for which air-dried samples were attached on carbon adhesive tabs (EMS Washington USA) and subsequently sputter coated with 15 nm Iridium (SCD500 Leica, Vienna, Austria). Crystal structure of the sample was confirmed by X-ray diffraction (XRD, Philips, The Netherlands, Cu-Kα, 30 kV, 50 mA). The stride length Å = 1.5406 λ (λ is the wavelength of X-ray radiation) and scanning angle (2θ) was in the range from 5° to 100°, with a step size of 0.02° and a measurement time of 1 s per step. Nitrogen gas adsorption isotherms were collected at 77 K (−196 °C) using a surface area and porosity analyzer (TriStar 3000, Micromeritics, USA). The Brunauer–Emmett–Teller (BET) model, Barrett–Joyner–Halenda (BJH) model and *t*-plot model were used to determine the specific surface area, pore diameter, and micropore volume individually. Prior to collecting the isotherms, samples were degassed at 300 °C for 2 h under a nitrogen gas flow of 30 ml/min in a degassing apparatus (SmartPrep 065, Micromeritics, USA).

2.4.3. UPLC analysis

UPLC (ultimate 3000, Thermo, USA) with a diode array detector (DAD) was used to determine the concentration of PhACs. UPLC is equipped with CSH phenyl-Hexyl column (3.5 mm, 300 Å, 0.1 × 150 mm). The mobile phase was a mixture of A (water with 0.1% formic acid) and B (acetonitrile with 0.1% formic acid) with a flow rate at 0.3 ml/min. The percentage of B gradually increased from 0% at 0.5 min to 80% at 13 min, kept constant for 3 min, then decreased to 0% at 17 min and stopped at 22.4 min. The sample injection volume was 10 μl. Detection results were acquired and analysed automatically by software. Limits of detection of PhACs were 50 μg/l and detection results of the standards showed a good linearity ($R^2 > 0.999$).

2.4.4. Toxicity assay

Green algae, blue-green algae (cyanophyta) and luminescence bacteria, typical microorganisms, were exposed to PhACs samples collected at different irradiation time points to determine the acute and chronic toxicity of PhACs. Toxicity assays were completed based on the 96-wells plate experiment and detected by a plate reader (Tecan infinite M200 PRO, Switzerland). Green algae *Pseudokirchneriella subcapitata* and blue-green algae *Anabaena flos-aquae* were obtained from Department of Aquatic Ecology and Water Quality Management, Wageningen University, The Netherlands; luminescence bacteria *Vibrio fischeri* was purchased from Microlan (The Netherlands). Algae were cultivated in an incubator shaker (Innova® 44, Eppendorf, USA, 600 lux, light/dark = 16 h/8 h, 20 °C, 80 rpm) and were fed with WC growth medium [23] weekly.

The growth inhibition of algae represents related toxicity of PhACs. Fluorescence of algae (excitation wavelength of 445 nm; emission wavelength of 680 nm) was applied to indicate their cell density, since the fluorescence of chlorophyll is in proportion to the density of algae cells [24,25]. Prior to the assay, a linear relationship of fluorescence and cell density was observed by using a cell counter (CASY Model TT, Roche, USA). Algae observed in the exponential growing phase were exposed to PhACs samples for 72 h, based on the method described by Blaise and Férard [26]. Inhibition of *V. fischeri* was analyzed based on the decay in emitted light when exposed to toxic compounds. The luminescence was recorded after 15 min exposure at room temperature in darkness. The inhibition was calculated following the established protocol offered by sub-department of Toxicology, Wageningen University, The Netherlands. For the mentioned toxicity assays, $CuSO_4$ as Cu (II) was selected as the reference compound to validate the protocols (Fig. A.2). Filtrated WWE was set as the blank control.

2.5. Photodegradation kinetics and effect of light attenuation

When TiO_2 was applied as the catalyst, photocatalysis kinetics of organic compounds fit the Langmuir–Hinshelwood model [27], which could be used to describe the reactions between radicals and substrate molecules in either absorbed or dissolved status [28].

$$-\frac{dC}{dt} = \frac{k_r KC}{1 + KC} \tag{1}$$

where k_r is the true photodegradation rate of the organic compound (mg/l/h), C the concentration of the compound (mg/l), t the illumination time, and K the adsorption coefficient of the compound to be degraded (l/mg). k_r related to several parameters such as mass of catalyst, efficient photon flow, layer of oxygen, etc. [29]. The L–H model can be simplified to a pseudo-first-order kinetic equation and k is the apparent rate of the pseudo-first-order reaction.

$$-\frac{dC}{dt} = k_r KC = kC \tag{2}$$

In addition, direct photolysis also follows the pseudo-first-order reaction [30]. The photodegration half-life of PhACs could be calculated by

$$t_{1/2} = \frac{\ln 2}{k} \tag{3}$$

In this study, removal of PhACs by adsorption onto immobilized TiO_2 in the dark was insignificant (Fig. A.3), showing that the removal of PhACs in our experiments can be attributed to photodegradation. In surface waters, photodegradation efficiencies are limited by light attenuation by depth [31]. Furthermore, it is reported that the pseudo-first-order kinetic constant of the contaminant is directly proportional to photon fluence underneath the water in direct photolysis [32–34]. The vertical profiles of down-welling attenuation can be estimated by the Lambert–Beer equation [35].

$$I_z = I_0 e^{-k_d z} \tag{4}$$

where I_0 *is* the light intensity at water surface measured by the upper sensor (photosynthetically active irradiation, μmol photons/(m^2 s)), z the depth underneath the water surface (m), I_z the light intensity at depth z, and k_d the light attenuation coefficient (m^{-1}). Therefore, for individual compounds, the photodegradation kinetic constant is connected with light intensity as in Eq. (5).

$$k = pI_z = pI_0 e^{-k_d z} \tag{5}$$

where p is the proportion constant. The value of k_d was determined by detecting light intensity at different water depths (Fig. A.4). The

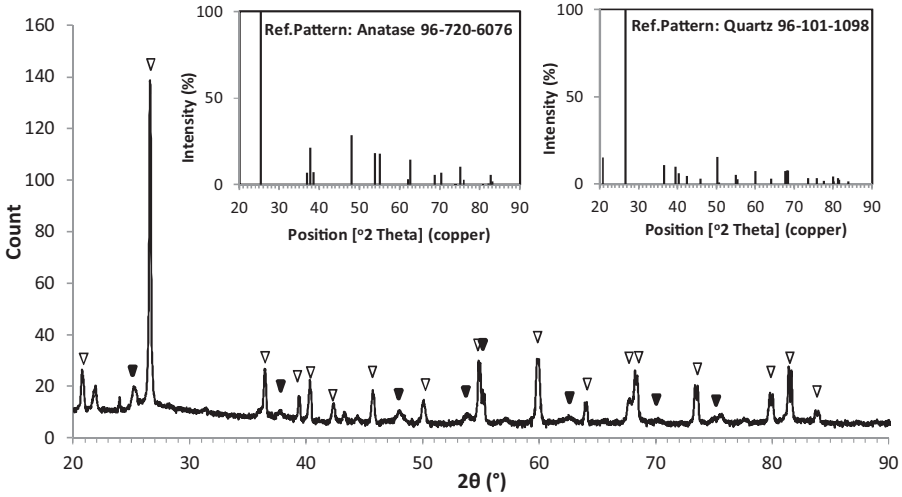

Fig. 1. XRD pattern of the immobilized TiO_2 on sand shows the peaks of anatase phase (close triangle) and quartz phase (open triangle).

slope of $ln\ (I/I_0)$ versus water depth gives a k_d value of $-3.17\ m^{-1}$ in DI.

3. Results and discussion

3.1. Characteristics of the immobilized catalyst

Various catalyst support materials have been used to enhance the available surface area of immobilized TiO_2 for PhACs removal, including glass spheres [36], glass slides [37], silicon plates [38], titanium alloys [39], fiber sheets [40], and activated carbon [41]. In this work, immobilization of TiO_2 on sand was investigated as a potential low-cost and robust catalyst.

The XRD pattern of the immobilized catalyst shows the presence of anatase and quartz phase, and the absence of impurities (Fig. 1). The characteristic diffraction peaks of TiO_2 can be observed at $2\theta = 25.4^\circ$ corresponding to the reference plane of anatase, which indicates TiO_2 was impregnated in the immobilized material. The anatase phase was produced on purpose during immobilization because this specific phase is preferred over other phases of TiO_2 for solar cell application due to its higher electron mobility, lower dielectric constant, lower density and lower deposition temperature [17]. In addition, the relative intensity of quartz peaks detected was the same as the reference plane, suggesting that the immobilization of TiO_2 did not change the structure of the sand. XRD results showed 68.2% of anatase crystalline phase compared with 31.8% of quartz phase. The crystallite size of anatase phase (D, nm) could be estimated by Scherrer's formula [42,43].

$$D = \frac{0.9\lambda}{\beta \cos\theta} \quad (6)$$

where λ is the wavelength of X-ray radiation (0.154 nm for Cu K_α used), θ the diffraction peak angle, and β the difference between the full width at half-maximum of detected sample and the standard sample at certain θ. The crystallite size of anatase was calculated to be 22.6–46.4 nm.

SEM images in Fig. 2 were taken at 100,000× magnifications to observe the surface morphology of quartz sand before and after immobilization of TiO_2. SEM images showed the relatively smooth surface of sand without obvious pores (Fig. 2a). After immobilization, spherical morphologies of TiO_2 grains were observed to be heterogeneously distributed on the sand surface (Fig. 2b). Microstructure of catalyst did not change after being used twice in the photodegradation experiment. According to the nitrogen gas adsorption isotherms, immobilization of TiO_2 increased the specific surface area of raw sand from 0.04 to 2.02 m^2/g. The expected increase was consistence with the morphology showed in SEM. Additionally, the micropore volume of sand increased from almost zero to 0.003 cm^3/g after immobilization. With the low micropore volume and small pore size (6.88 nm in diameter), the immobilized catalyst was expected not to adsorb PhACs, which was supported by the results obtained from adsorption tests (Fig. A.3).

3.2. Light attenuation by water: relation between depth and photolysis efficiency

In order to study the application of solar irradiation in passive photodegradation of PhACs, we investigated the effect of light attenuation by water depth on the photodegradation performance. PhACs samples were collected at different water depths every 24 h. However, counting the detection deviation, there was

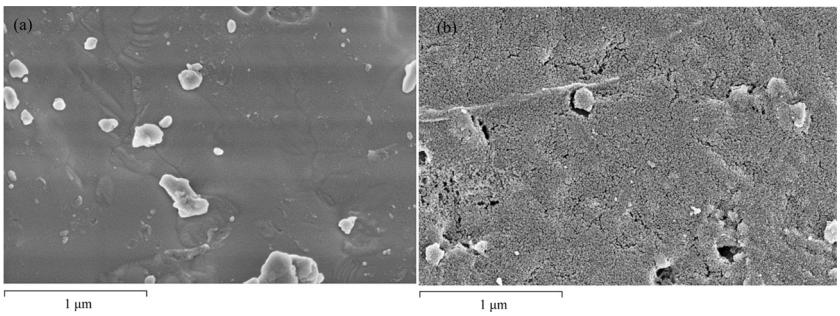

Fig. 2. SEM images of (a) surface of raw sand (200–500 μm); (b) spherical morphologies of TiO_2 grains distributed on the surface of one sand particle.

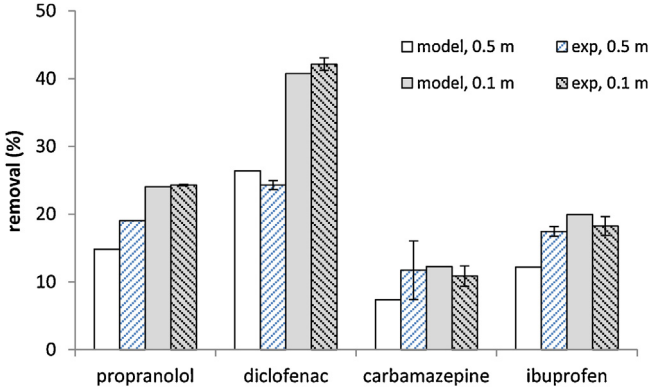

Fig. 3. Comparison of removal efficiencies of individual PhACs from modelling and experimental set-ups. 96 h photolysis of 5 mg/l PhACs each, spiked in deionized water (DI). Error bars indicate standard errors of the mean (s.e.m.), $n = 2$.

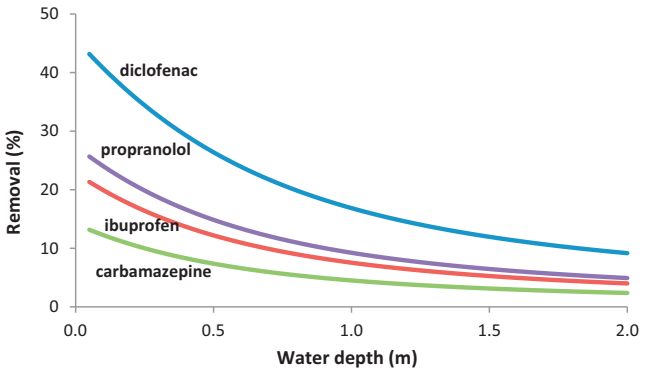

Fig. 4. Relationship of PhACs removal versus water depth obtained from validated modelling, 96 h direct photolysis of PhACs spiked in deionized water (DI). Relatively higher removal efficiency corresponded to a depth less than 1.0 m.

no obvious concentration difference (<3%) between samples at different water depths in 0.5 m column experiment. Thus, we developed a simplified model to establish the relationship between the pseudo-first-order constant of individual PhACs with water depths. According to the Eq. (2) and (5), we calculated $\bar{C}_{t,model}$, the average concentration of PhACs in the column at certain time points in the model as follows,

$$\bar{C}_{t,\mathrm{model}} = \frac{1}{H}\int_0^H C_0 e^{-kt}dz = \frac{1}{H}\int_0^H C_0 e^{-pI_z t}dz$$

$$= \frac{1}{H}\int_0^H C_0 e^{-pI_0 e^{-k_d z}t}dz \quad (7)$$

where H is the total depth of the water column. The experimental value of $\bar{C}_{t,\mathrm{exp}}$ could be obtained by mixing the samples collected at different water depths at certain time points.

In order to yield a more accurate simulation, we simulated and experimentally tested two scenarios: direct photolysis of four PhACs in a water column of 0.1 m depth in the beaker and 0.5 m depth in the column. We iterated different values of the proportion constant p to minimize the variance between $\bar{C}_{t,model}$ and experimental $\bar{C}_{t,\mathrm{exp}}$. According to the modelling results, p was 0.021 for PRO, 0.040 for DFC, 0.010 for CBZ, and 0.017 for IBP. By integrating the Eq. (5), pseudo-first order constants could be calculated.

$$k_{model} = \frac{1}{H}\int_0^H pI_0 e^{-k_d z}dz \quad (8)$$

According to the Eq. (2), the removal efficiencies of PhACs can be calculated using kinetic constants. Then the calculated removal efficiencies were compared with related experimental results (Fig. 3).

In Fig. 3, the modelling results indicate high similarity in removal efficiencies of four PhACs compared to the efficiencies obtained from experiments performed at water depth of 0.5 m and 0.1 m, respectively. Additionally, according to the regression analysis in Fig. A.5, the modelling concentrations of four PhACs are approximate to the related experimental values. Thus, the model describes the experimental results adequately, indicating the proposed attenuation mechanisms to be active. Furthermore, we could predict the relationship between water depth and direct photolysis removal efficiency of individual PhACs (Fig. 4). The data presented here did not account for the water quality containing various components and other site-specific factors, but only focused on the direct photolysis of PhACs. Results suggest that removal of PhACs by direct photolysis distinctly decreased with water depth when the depth is less than 1.0 m, while the removal efficiencies are insignificant when the water column is deeper than 1.0 m (Fig. 4). However, for the natural attenuation of PhACs in waters, as calculated by our work, even the water depth was close to 0, the removal efficiencies were still not satisfying, with approximately 26% for PRO, 43% for DFC, 13% for CBZ, and 21% for IBP. Therefore, it is essential to apply a catalyst to improve the photodegradation performance. For the following kinetic study, we completed the experiment by applying a water depth of 0.1 m to achieve higher removal performance based on our experimental set-up.

3.3. Photodegradation performance, kinetics and mechanisms

Following the optimized water depth, we evaluated the effect of immobilized TiO_2 on PhACs removal in a simplified system, which is performing photolysis and photocatalysis in DI for 96 h. With respect to the PhACs spiked in DI, both photolysis and photocatalysis of PhACs fit the pseudo-first-order kinetics and the slope represents the kinetic constant (Fig. A.7). However, photocatalysis showed notably better performance in eliminating PhACs than photolysis (Fig. 5). The half-life time of PRO and DFC under simulated solar irradiation were decreased from 239 and 121 h to 13 and 12 h due to addition of the catalyst (Table 1). The less photo-active PhACs, CBZ and IBP showed long half-lift times (578 h for CBZ; 330 h for IBP) under photolysis (Table 1), which is comparable to a study by Matamoros et al. [44], in which CBZ and IBP were exposed to solar light in May in Barcelona. However, for photocatalysis, the half-life time of CBZ and IBP were only 25 and 21 h, indicating a good performance of the catalyst, which was also confirmed by the formation of by-products detected by UPLC. Chromatography results showed more by-products formed and further degraded in photocatalysis than in photolysis (Fig. A.6), indicating the process of photocatalysis was much faster. Thus, by producing more active hydroxyl radicals (•OH), the immobilized catalyst showed significant enhancement for removing PhACs.

To understand and determine the effect of immobilized TiO_2 in a real water matrix, the catalyst was applied in the WWE. In WWE, photocatalysis of PhACs also performed better than photolysis (Fig. 5). Although catalyst addition yielded a smaller improvement in removal efficiencies in WWE when compared with the DI photodegradation, the removal efficiencies of PRO, DFC, CBZ, and IBP were 100%, 100%, 76%, and 74% respectively after 96 h photocatalysis (Table 1). Especially for the PhACs recalcitrant towards biodegradation, PRO, DFC and CBZ, photocatalysis under simulated solar light showed considerable removal performance. Additionally, the formation and depletion of by-products in photocatalysis was faster compared with photolysis (Fig. 6). For example, the by-product at 10.03 min in the chromatogram was produced within 24 h irradiation and depleted after 72 h in photocatalysis, while it only appeared and accumulated after 48 h irradiation in photolysis.

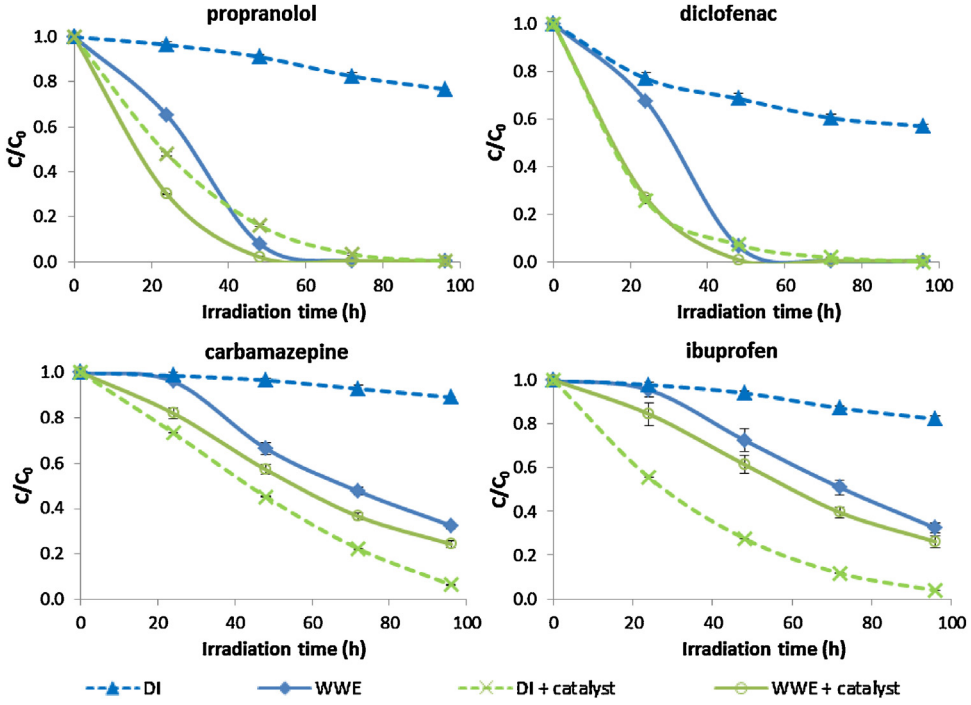

Fig. 5. Photolysis and photocatalyis of PhACs versus irradiation time. 5 mg/l for each PhAC spiked in deionized water (DI) and wastewater effluent (WWE) under 96 h simulated solar irradiation. Data points and error bars are average values/standard errors of the mean (s.e.m.), $n = 2$.

Table 1
Pseudo-first-order kinetic constants and removal performance of PhACs under 96 h photolysis and photocatalysis. 5 mg/l for each PhAC spiked in deionized water (DI) and wastewater effluent (WWE).

Matrix	PhACs	Photolysis				Photocatalysis			
		removal (%)	k(h^{-1})	r^2	$t_{1/2}$(h)	removal (%)	k(h^{-1})	r^2	$t_{1/2}$(h)
DI	Propranolol	23.3 ± 0.1	−0.0029	0.98	239.0	99.8 ± 0.2	−0.0523 ± 0.0088	0.96	13.3
	Diclofenac	43.3 ± 0.9	−0.0057 ± 0.0001	0.92	121.6	100	−0.0562 ± 0.0022	1.00	12.3
	Carbamazepine	10.9 ± 1.5	−0.0012 ± 0.0001	0.97	577.6	93.5 ± 0.1	−0.0277 ± 0.0002	0.93	25.0
	Ibuprofen	17.7 ± 1.4	−0.0021 ± 0.0001	0.96	330.1	96.1 ± 0.2	−0.0336 ± 0.0003	0.98	20.7
WWE	Propranolol	100	−0.0527 ± 0.0003	0.87	13.2	100	−0.0808 ± 0.0027	0.95	8.6
	Diclofenac	100	−0.0573 ± 0.0005	0.85	12.1	100	−0.1018 ± 0.0033	0.93	6.8
	Carbamazepine	67.4 ± 2.2	−0.0122 ± 0.0007	0.96	57.0	75.6 ± 2.6	−0.0150 ± 0.0008	0.98	46.2
	Ibuprofen	67.6 ± 1.4	−0.0119 ± 0.0005	0.94	58.2	73.8 ± 1.6	−0.0142 ± 0.0006	0.98	48.8

Photolysis constants of PhACs in WWE were upwards of ten times higher compared with the related values in DI. For PRO and DFC in DI, the high constants were even comparable with the constants obtained when the catalyst was present (Table 1). This is possibly caused by the enhancement of degradation by dissolved organic matter (DOM) in WWE (DOM = 12.2 mg C/l), which could absorb light to excite triplet states of DOM (^{3}DOM*) and further to •OH. •OH could subsequently oxidize PhACs into by-products or CO_2, shown as the mechanism 4 in Fig. 7 and further elaborated below. ^{3}DOM* could enhance the transformation of aquatic contaminants by acting as a photosensitizer [45], especially for aromatic pollutants with a phenolic OH group [46], such as PRO in our case (Table A.1). Chen et al. [47] verified fulvic acid, a generic form of DOM, to be the main photochemically reactive species to interact with PRO. The kinetic constant of PRO increased from 0.069 h^{-1} to 0.230 h^{-1} after adding fulvic acid (5 mg C/l). In addition, the first order constant of DFC proved to increase twice higher under UV irradiation after adding effluent organic matter of 10.2 mg C/l from a WWTP in Korea [48].

Nitrate could adsorb solar light when λ < 350 nm [49] and produce •OH to accelerate the indirect photodegradation of PhACs. Compared with DOM, the light screening effect of nitrate is negligible with its very low molar extinction coefficient [50]. Ji et al. [51] reported an enhanced photodegradation rate constant of atenolol from 0.001 min^{-1} to 0.007 min^{-1}, when the concentration of nitrate increased from 0.5 mM/l to 10 mM. In this study, the concentration of WWE was 0.07 mM/l (Table A.2), much lower than the level in previous literature studying the effect of nitrate on micropollutants removal. Thus, the presence of nitrate might insignificantly contribute to enhancing photodegradation of PhACs.

On the other hand, DOM and other inorganic ions including CO_3^{2-} and HCO_3^- could inhibit the photodegradation. DOM is the main inhibitor while inorganic ions contribute insignificant to scavenging [52]. There are three main mechanisms by which DOM can inhibit photodegradation, that is (1) DOM acts as a quencher of reactive species such as •OH; (2) DOM screens photo-chemically active light; or (3) DOM reacts with contaminant intermediates (Fig. 7).

For the first proposed mechanism, in our case with 12.2 mg C/l DOM, the first mechanism might be negligible, because no significant •OH quenching effect (>10%) on aromatic ketones was detected when the concentration of DOC was below 22–72 mg/l [53].

As discussed in Section 2.5, photodegradation of PhACs in this study followed pseudo-first order kinetics, which means an exponential decrease of the concentration of PhACs in time. However, in the case of photolysis in WWE, completed exponential tendencies were not detected for all the PhACs due to an apparent delay

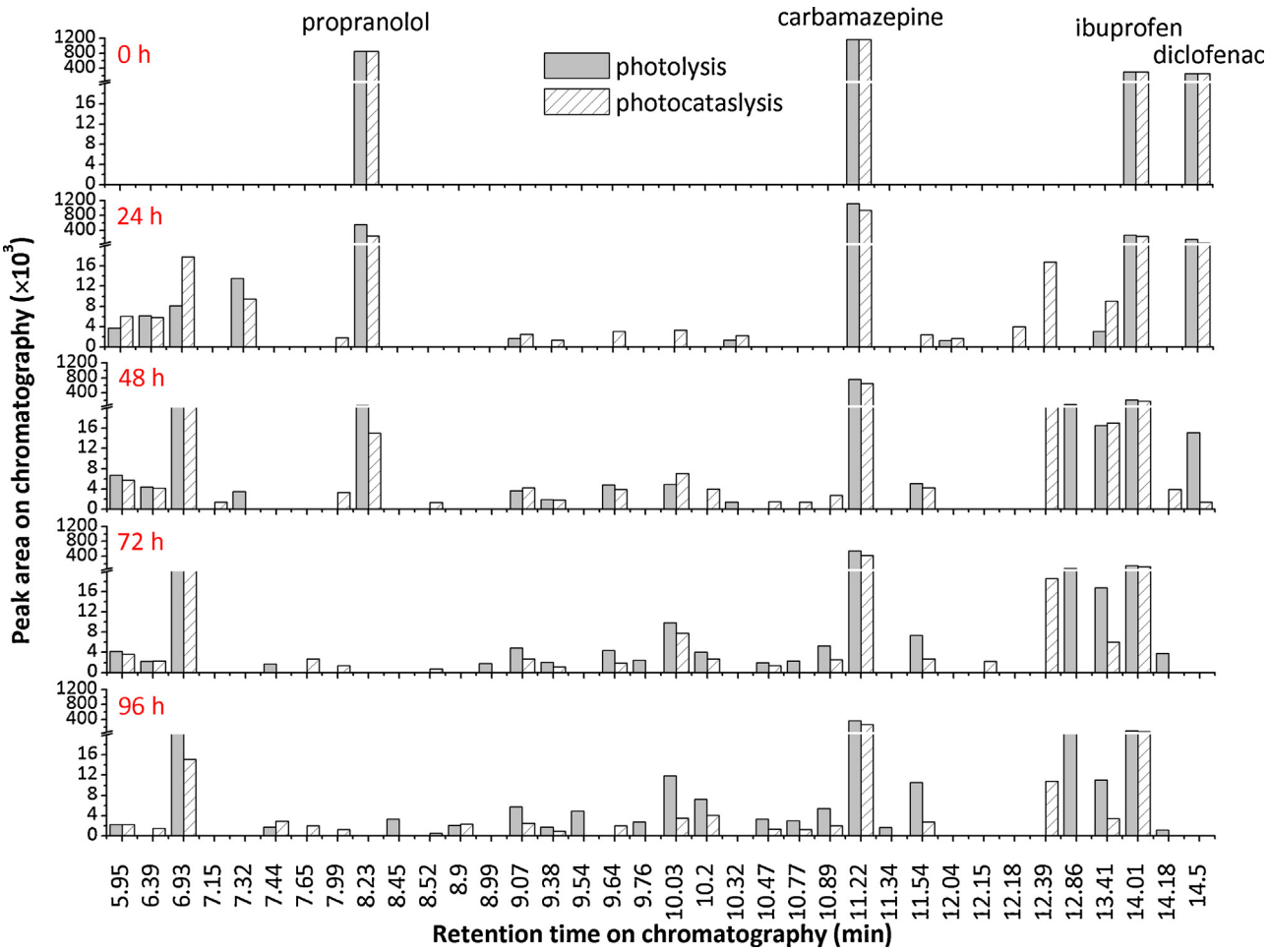

Fig. 6. Presence and variation of by-products at different irradiation time points showed in chromatography spectrum. Photolysis and photocatalysis of PhACs spiked in wastewater effluent (WWE).

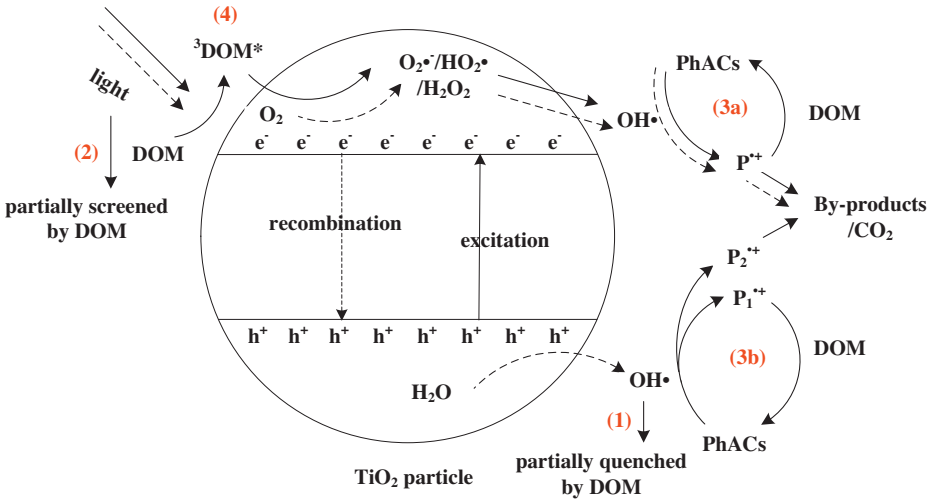

Fig. 7. Hypothetical mechanisms of photocatalysis of PhACs (P) without DOM (dash lines), and the role of DOM as the photosensitizer and inhibitor (solid lines). The inhibition of DOM could be due to (1) quenching •OH; (2) screening active photons; (3) reacting with oxidized PhACs ($P^{\bullet+}$ or $P_1^{\bullet+}$). The enhancement of DOM could be due to (4) production of $^3DOM^*$ and further to •OH.

phase observed in the first 24 h (Fig. 5). This might be caused by the light screening of DOM present in WWE (Fig. 7), which is the second proposed mechanism. DOM has a colored or chromophore fraction which could absorb solar light and modify the spectrum of radiation penetrating into the water column [54]. Similarly, the same phenomenon was also observed by Dong et al. [55], in which the photodegradation of atenolol, carbamazepine, and primidone in WWE was delayed in the first 24 or 48 h under solar irradiation.

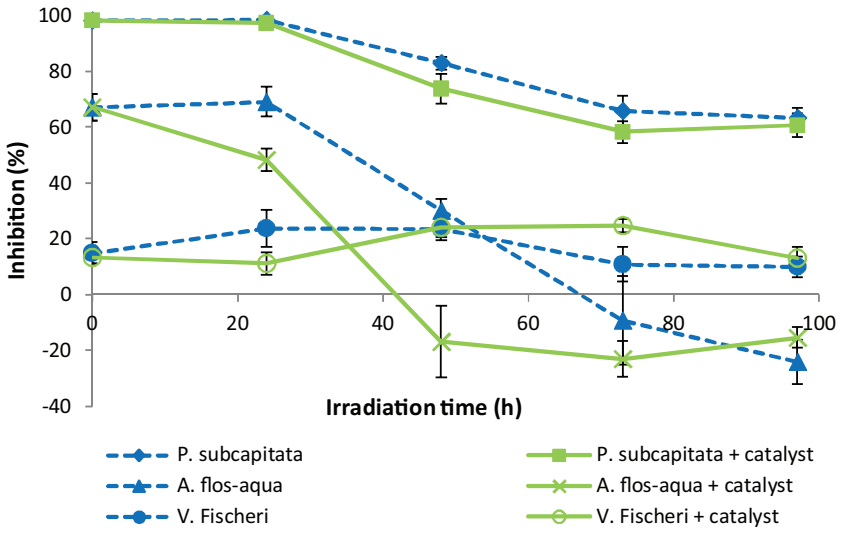

Fig. 8. Toxicity of PhACs spiked in wastewater effluent (WWE) during photocatalysis and photolysis. 5 mg/l for each PhAC under 96 h simulated solar irradiation. Green algae (*Pseudokirchneriella subcapitata*) and blue-green algae (*Anabaena flos-aqua*) exposed to PhACs for 72 h in algae incubator; luminescence bacteria (*Vibrio fischeri*) exposed for 15 min. Data points and error bars are average values/standard deviation, $n = 5$.

After the delay phase, production of •OH appeared to be dominant and photodegradation proceeded at an increasing rate. The delay phase was much shorter or absent in case photocatalysis was applied, and this is consistent with the higher amounts of radicals produced by the catalyst.

In the third proposed mechanism, after reacting with •OH or ^{3}DOM*, PhACs transform to a radical cation, $P^{\bullet+}$ (in the case of transferring one electron) or to different types of intermediate radical cations such as $P_1^{\bullet+}$ and $P_2^{\bullet+}$, shown as path 3a and 3b in Fig. 7. A portion of $P^{\bullet+}$ could either be further irreversibly transformed to by-products or to CO_2 (as in $P_1^{\bullet+}$), or be reduced by DOM to reform the parent compounds (as in $P_2^{\bullet+}$) [32,56]. DOM contains a variety of organic moieties, especially the phenolic functional groups which could act as antioxidants to reduce the oxidation intermediates $P^{\bullet+}$ [56]. This process was shown by investigating the photo-depletion of 22 contaminants in a photoreactor installed with a mercury lamp [45]. They found that the depletion rate of half of the target contaminants decreased in the presence of Suwannee River fulvic acid which was used as their reference DOM.

In WWE, when more •OH were produced by the catalyst, the first-order constants of PRO and DFC increased, while the constants of CBZ and IBP were almost the same with those in photolysis (Table 1). However, when the catalyst was present, CBZ and IBP have the potential to be further degraded, as the removal efficiencies of those two compounds yielded higher level in DI compared with WWE. As the inhibition of DOM through mechanism 1 and 2 are identical for all the PhACs in mixture, the different levels of inhibition between different PhACs were possibly caused by mechanism 3. It is reported that DOM mediated indirect photolysis of organic compounds is partly driven by the chemical reactivity of the contaminants [57]. In our work, during the competition of •OH with the other PhACs in DI photocatalysis experiment, CBZ and IBP are more recalcitrant to degradation. Thus, intermediate radical cations of CBZ and IBP ($P^{\bullet+}$) could be more easily reduced back to their parent compounds. We hypothesize that the intermediate radical cations of CBZ and IBP have been selectively reformed to parent compounds through reduction by DOM, which is in line with mechanism 3b. That means no matter how much $P_1^{\bullet+}$ is produced by reactive species, $P_1^{\bullet+}$ will be reduced to P by sufficient DOM while the production of irreversible by-products could only depend on the production of $P_2^{\bullet+}$, resulting in no increase of kinetic constants of CBZ and IBP even though the catalyst provides more reactive species. However, for PRO and DFC, we could not conclude whether DOM inhibited their depletion rates because their kinetic constants in WWE photocatalysis were higher compared with the constants in DI photocatalysis. Assuming similar DOM inhibition for PRO and DFC, the story might be different from that of CBZ and IBP. When more $P^{\bullet+}$ is produced due to catalysis, even though parts of the $P^{\bullet+}$ were transformed to parent PRO and IBP, there were still more by-products formed because of the excessive $P^{\bullet+}$ (Fig. 7). This conforms to mechanism 3a. Wenk et al. [56] also showed that the theory of $P^{\bullet+}$ fits for sulfamethoxazole while the theory of $P_1^{\bullet+}$ and $P_2^{\bullet+}$ is suitable for N, *N*-dimethylaniline and trimethoprim, when 5 μM of the components are exposed to a mercury lamp with DOM in 0.1–2.9 mg C/l.

It is reported that the DOM type in WWE greatly varies among different water treatment systems, hence unexpected inhibitions of oxidation might occur [58]. Alternatively natural waters and wetland DOM might enhance photodegradation of PhACs otherwise conservative in degradation [48]. In order to understand the relationship between the DOM structure and its potential role in photodegradation, we performed FTIR analysis of the WWE solid. From the FTIR spectra in Fig. A.8, we found absorption bands that correspond to the following functional groups [59,60]: (1) 3352 cm^{-1} (O—H stretching of inter- and intra-molecular hydrogens bonds); (2) 1638 cm^{-1} (aromatic C=C skeletal vibrations, asymmetric stretching of C=O of quinones and ketones, symmetric stretching of COO^-); (3) 1406 cm^{-1} (asymmetric stretching of COO^-, C—H bending of aliphatic groups); (4) 1188 cm^{-1} (C—O asymmetric stretching and OH bending of COOH groups and phenols); (5) 1101 cm^{-1} C—O stretching of primary alcohols and in-plane bending of aromatic C—H. These results show the presence of aromatic and phenolic functional groups, and this might explain the complicated role of DOM in photodegradation not only as a photosensitizer, but also as an inhibitor for PhACs photodegradation. DOM could produce ^{3}DOM* under irradiation, which could enhance the transformation of aquatic contaminants by acting as a photosensitizer [45]. However, it is also reported that highly aromatic DOM generally presents a higher efficiency in inhibiting ^{3}DOM*-induced oxidation and a lower photochemical reactivity. Furthermore, phenolic functional groups

could act as antioxidants to reduce the oxidation intermediates $P^{\bullet+}$ [56].

3.4. Toxicity and biodegradability

In order to evaluate the feasibility and environmental impact of the photodegradation for treating WWE spiked with PhACs, toxicity tests were performed in parallel with sampling for PhACs. It is reported that non-stable by-products formed during photodegradation may pose environmental risks [61]. Therefore, the toxicity of PhACs during photodegradation is essential when assessing the feasibility of water treatment techniques.

We used known aquatic microorganisms, including green algae, blue-green algae, and luminescence bacteria, to test the chronic (72 h exposure for algae species) and acute (15 min exposure for bacteria) toxicity of PhACs spiked in WWE. Previous studies mainly focus on the toxicity of parent compounds [62], synergistic toxicity of PhACs and related by-products before and after photodegradation [63], or toxicity of PhACs during photodegradation in DI rather than the real water matrix [64].

The inhibition of microorganisms was calculated by setting WWE without spiking PhACs as the blank control. In Fig. 8, the presence of PhACs indeed inhibited the target microorganisms, among which the green algae seemed to be more sensitive to the PhACs with almost 100% growth inhibition before photodegradation. During 96 h irradiation, chronic toxicity of PhACs to the algae species decreased. Similarly, in the work of Rizzo et al. [65], the toxicity of mixed PhACs (10 mg/l amoxicillin, 5 mg/l CBZ, 2.5 mg/l DFC) to *P. subcapitata* gradually decreased from 96% to 60% inhibition when the PhACs were degraded by UV irradiation for 2 h. For the blue-green algae, a dramatic decrease in toxicity was achieved yielding negative inhibition, i.e., a slight stimulation. This fact might be because residual CBZ, IBP, and the photodegradation by-products (Fig. 6) are mildly toxic or non-toxic, while the high content of organic matter in WWE is available for the cells as a nutrition resource resulting in growth. This enhanced growth of blue-green algae was also found in the control wells filled with WWE only. For the luminescence bacteria, the produced intermediates seemed to be similarly toxic than the parent compounds during the photodegradation, followed by a slight decreased tendency.

Overall, the algae growth inhibition assays suggested that photocatalysis promoted the formation of less toxic by-products and the toxicity decreased with prolonging treatment time. Additionally, photocatalysis caused a more obvious reduction of toxicity compared with photolysis. On the basis of the results, we could conclude that the photocatalysis technique not only yielded high PhACs removal efficiencies, but also led to a reduction in the toxicity after treatment.

In practical cases, PhACs could be further degraded downstreams in natural water systems, such as natural wetlands, ponds or lagoons before discharge to lakes and rivers [66]. In order to evaluate the suitability of the photocatalytic treatment in wastewater containing PhACs, biodegradability (BOD_5/COD) was assessed before and after photolysis and photocatalysis. After spiking 5 mg/L PhACs of each, COD of WWE increased by 31.8 mg/l while BOD_5 increased by 6.7 mg/l (Table 2), suggesting that only a small fraction of PhACs have the potential to be metabolized by bacteria within test period of BOD_5. Moreover, the BOD_5/COD ratio was lower than 0.20, which means the WWE containing PhACs was hardly biodegradable [67], thus preventing the direct application of bio-treatment techniques. After photocatalysis, COD decreased due to the mineralization of PhACs into by-products or CO_2. Comparison of COD levels after photolysis and photocatalysis indicates that photocatalysis removed organic matter more efficiently. However, BOD_5 did not show an obvious increase following either treatment. Even though some by-products were more completely degraded during the photocatalysis, 18 different by-products were detected at the end (Fig. 6). These residual by-products were not easily photo-degradable under the experimental conditions in our work. Overall, the decrease of toxicity and slight increase of biodegradability showed that photocatalysis has the potential to improve the susceptibility of effluent to further biodegradation in natural surface water systems such as wetlands and lagoons.

Table 2
Biodegradability of wastewater effluent (WWE) before and after being treated by photolysis and photocatalysis.

Conditions	BOD_5 (mg/l)	COD (mg/l)	BOD_5/COD
WWE	6.0 ± 1.0	35.2 ± 0.6	0.17
WWE spiked with mixed PhACs	12.7 ± 0.3	67.0 ± 2.8	0.19
After photolysis treatment of spiked WWE	12.7 ± 0.1	61.9 ± 1.6	0.19
After photocatalysis treatment of spiked WWE	13.7 ± 2.7	46.6 ± 3.0	0.29

4. Conclusions

The photolysis and photocatalysis of four selected PhACs spiked in WWE, has been demonstrated under simulated solar irradiation. The photodegradation pattern followed pseudo-first order kinetics. By using the immobilized TiO_2 on sand as the catalyst, removal efficiencies of PhACs were significantly improved in DI. In the case of WWE, the removal rates of PRO and DFC were higher in photocatalysis than in photolysis; the rates of CBZ and IBP did not obviously increase. However, the degradation of PhACs to form by-products and further degradation of these by-products were faster in photocatalysis compared with photolysis. DOM could enhance the photodegradation efficiency by producing more reactive species, while it could also inhibit the degradation performance. A possible mechanism contributing to this is a partial or selective reduction of the oxidized PhACs back to parent compounds. After photocatalysis, the chronic toxicity of PhACs decreased for the aquatic microorganisms, green algae and blue-green algae. In addition, the biodegradability of WWE spiked with PhACs was slightly improved.

From a perspective of application, the photocatalysis was performed by combining the economical and robust components including TiO_2, sand, and solar light. Additionally, photocatalysis under simulated solar light showed considerable removal performance for the PhACs recalcitrant towards biodegradation, PRO, DFC and CBZ. Therefore, applying the photocatalysis in an open shallow treatment cell as a post-treatment technique would be beneficial for the attenuation of PhACs in the downstream located natural water systems, such as wetlands, lagoons, or surface waters.

Acknowledgements

Authors thank Harry Bruning for helpful modelling discussion, Tinka Murk and Ziqiu Su for the assistance of toxicity assays. The support provided by China Scholarship Council (CSC) during a study of Yujie He in Wageningen University is acknowledged.

Appendix A. Supplementary data

Supplementary data associated with this article can be found, in the online version, at http://dx.doi.org/10.1016/j.apcatb.2015.09.015.

References

[1] C. Martinez, S. Vilarino, M.I. Fernandez, J. Faria, M. Canle, J.A. Santaballa, Appl. Catal. B 142 (2013) 633–646.
[2] M. Gros, M. Petrovic, A. Ginebreda, D. Barcelo, Environ. Int. 36 (2010) 15–26.
[3] M.J. Focazio, D.W. Kolpin, K.K. Barnes, E.T. Furlong, M.T. Meyer, S.D. Zaugg, L.B. Barber, M.E. Thurman, Sci. Total Environ. 402 (2008) 201–216.
[4] V. Matamoros, J. García, J.M. Bayona, Water Res. 42 (2008) 653–660.
[5] K. Kummerer, Annu. Rev. Environ. Resour. 35 (2010) 57–75.
[6] R. Andreozzi, M. Raffaele, P. Nicklas, Chemosphere 50 (2003) 1319–1330.
[7] I. Oller, S. Malato, J.A. Sanchez-Perez, Sci. Total Environ. 409 (2011) 4141–4166.
[8] S. Canonica, L. Meunier, U. Von Gunten, Water Res. 42 (2008) 121–128.
[9] V.J. Pereira, K.G. Linden, H.S. Weinberg, Water Res. 41 (2007) 4413–4423.
[10] V.J. Pereira, H.S. Weinberg, K.G. Linden, P.C. Singer, Environ. Sci. Technol. 41 (2007) 1682–1688.
[11] R.K. Szabo, C. Megyeri, E. Illes, K. Gajda-Schrantz, P. Mazellier, A. Dombi, Chemosphere 84 (2011) 1658–1663.
[12] N. Klamerth, L. Rizzo, S. Malato, M.I. Maldonado, A. Agüera, A.R. Fernández-Alba, Water Res. 44 (2010) 545–554.
[13] S. Miralles-Cuevas, I. Oller, A. Ruiz Aguirre, J.A. Sánchez Pérez, S. Malato Rodríguez, Chem. Eng. J. 239 (2014) 68–74.
[14] A. Grossberger, Y. Hadar, T. Borch, B. Chefetz, Environ. Pollut. 185 (2014) 168–177.
[15] J. Rivera-Utrilla, M. Sánchez-Polo, M.Á. Ferro-García, G. Prados-Joya, R. Ocampo-Pérez, Chemosphere 93 (2013) 1268–1287.
[16] Y. Zhang, S.-U. Geißen, C. Gal, Chemosphere 73 (2008) 1151–1161.
[17] O. Carp, C.L. Huisman, A. Reller, Prog. Solid State Chem. 32 (2004) 33–177.
[18] N. De la Cruz, R.F. Dantas, J. Gimenez, S. Esplugas, Appl. Catal. B 130 (2013) 249–256.
[19] K. Hund-Rinke, M. Simon, Environ. Sci. Pollut. Res. 13 (2006) 225–232.
[20] EEC, Off. J. Eur. Commun. 276 (1967) 1–98.
[21] D. Avisar, I. Horovitz, L. Lozzi, F. Ruggieri, M. Baker, M.-L. Abel, H. Mamane, J. Hazard. Mater. 244–245 (2013) 463–471.
[22] Q.B. Xia, Z. Li, H.X. Xi, K.F. Xu, Adsorpt. Sci. Technol. 23 (2005) 357–366.
[23] R.R.L. Guillard, C.J. Lorenzen, J. Phycol. 8 (1972) 10–14.
[24] A. Eisentraeger, W. Dott, J. Klein, S. Hahn, Ecotoxicol. Environ. Saf. 54 (2003) 346–354.
[25] P. Mayer, R. Cuhel, N. Nyholm, Water Res. 31 (1997) 2525–2531.
[26] C. Blaise, J.-F. Férard, Small-scale Freshwater Toxicity Investigations: Toxicity Test Methods, Springer, Dordrecht, 2005.
[27] T.E. Doll, F.H. Frimmel, Water Res. 38 (2004) 955–964.
[28] I.K. Konstantinou, T.A. Albanis, Appl. Catal. B 49 (2004) 1–14.
[29] A. Fernández, G. Lassaletta, V.M. Jiménez, A. Justo, A.R. González-Elipe, J.M. Herrmann, H. Tahiri, Y. Ait-Ichou, Appl. Catal. B 7 (1995) 49–63.
[30] M.J. García-Galán, M.S. Díaz-Cruz, D. Barceló, Water Res. 46 (2012) 711–722.
[31] V. Matamoros, A. Duhec, J. Albaiges, J.M. Bayona, Water Air Soil Pollut. 196 (2009) 161–168.
[32] S. Canonica, M. Freiburghaus, Environ. Sci. Technol. 35 (2001) 690–695.
[33] Q.-T. Liu, H.E. Williams, Environ. Sci. Technol. 41 (2007) 803–810.
[34] R.G. Zepp, D.M. Cline, Environ. Sci. Technol. 11 (1977) 359–366.
[35] W.C. Dennison, R.J. Orth, K.A. Moore, J.C. Stevenson, V. Carter, S. Kollar, P.W. Bergstrom, R.A. Batiuk, Bioscience 43 (1993) 86–94.
[36] N. Miranda-García, S. Suárez, B. Sánchez, J.M. Coronado, S. Malato, M.I. Maldonado, Appl. Catal. B 103 (2011) 294–301.
[37] M. Piecha, M. Sarakha, P. Trebse, J. Photochem. Photobiol. A 213 (2010) 61–69.
[38] S. Vilhunen, M. Bosund, M.-L. Kääriäinen, D. Cameron, M. Sillanpää, Sep. Purif. Technol. 66 (2009) 130–134.
[39] H.M. Coleman, E.J. Routledge, J.P. Sumpter, B.R. Eggins, J.A. Byrne, Water Res. 38 (2004) 3233–3240.
[40] R.R. Giri, H. Ozaki, S. Ota, R. Takanami, S. Taniguchi, Int. J. Environ. Sci. Technol. (Tehran) 7 (2010) 251–260.
[41] D. Keane, S. Basha, K. Nolan, A. Morrissey, M. Oelgemöller, J. Tobin, Catal. Lett. 141 (2011) 300–308.
[42] R.Q. Gao, X.M. Hou, Int. J. Min. Metall. Mater. 20 (2013) 593–597.
[43] D. Papoulis, S. Komarneni, D. Panagiotaras, E. Stathatos, K.C. Christoforidis, M. Fernández-García, H. Li, Y. Shu, T. Sato, H. Katsuki, Appl. Catal. B 147 (2014) 526–533.
[44] V. Matamoros, A. Duhec, J. Albaigés, J.M. Bayona, Water Air Soil Pollut. 196 (2008) 161–168.
[45] S. Canonica, H.U. Laubscher, Photochem. Photobiol. Sci. 7 (2008) 547–551.
[46] D. Vialaton, C. Richard, Aquat. Sci. 64 (2002) 207–215.
[47] Y. Chen, C. Hu, X. Hu, J. Qu, Environ. Sci. Technol. 43 (2009) 2760–2765.
[48] E. Lee, H.K. Shon, J. Cho, J. Hazard. Mater. 276 (2014) 1–9.
[49] F. Machado, P. Boule, J. Photochem. Photobiol. A 86 (1995) 73–80.
[50] Y. Chen, K. Zhang, Y. Zuo, Sci. Total Environ. 463–464 (2013) 802–809.
[51] Y. Ji, C. Zeng, C. Ferronato, J.-M. Chovelon, X. Yang, Chemosphere 88 (2012) 644–649.
[52] Y. Xu, T.V. Nguyen, M. Reinhard, K.Y.-H. Gin, Chemosphere 85 (2011) 790–796.
[53] J. Wenk, S.N. Eustis, K. McNeill, S. Canonica, Environ. Sci. Technol. 47 (2013) 12802–12810.
[54] J.F. Leal, V.I. Esteves, E.B.H. Santos, J. Environ. Chem. Eng. (2015).
[55] M.M. Dong, R. Trenholm, F.L. Rosario-Ortiz, J. Hazard. Mater. (2004).
[56] J. Wenk, U. von Gunten, S. Canonica, Environ. Sci. Technol. 45 (2011) 1334–1340.
[57] J. Guerard, P. Miller, T. Trouts, Y.-P. Chin, Aquat. Sci. 71 (2009) 160–169.
[58] A.L. Boreen, B.L. Edhlund, J.B. Cotner, K. McNeill, Environ. Sci. Technol. 42 (2008) 5492–5498.
[59] L.B. Barber, J.A. Leenheer, T.I. Noyes, E.A. Stiles, Environ. Sci. Technol. 35 (2001) 4805–4816.
[60] A. Traversa, E. Loffredo, C. Gattullo, A. Palazzo, T. Bashore, N. Senesi, J. Soils Sed. 14 (2014) 432–440.
[61] A. Agüera, L.A. Perez Estrada, I. Ferrer, E.M. Thurman, S. Malato, A.R. Fernandez-Alba, J. Mass Spectrom. 40 (2005) 908–915.
[62] J.M. Brausch, K.A. Connors, B.W. Brooks, G.M. Rand, Human pharmaceuticals in the aquatic environment. A review of recent toxicological studies and considerations for toxicity testing, Rev. Environ. Contam. Toxicol. (2012) 1–99.
[63] M.S. Diniz, R. Salgado, V.J. Pereira, G. Carvalho, A. Oehmen, M.A.M. Reis, J.P. Noronha, Sci. Total Environ. 505 (2015) 282–289.
[64] L. Rizzo, S. Meric, D. Kassinos, M. Guida, F. Russo, V. Belgiorno, Water Res. 43 (2009) 979–988.
[65] L. Rizzo, S. Meric, M. Guida, D. Kassinos, V. Belgiorno, Water Res. 43 (2009) 4070–4078.
[66] J.L. Conkle, J.R. White, C.D. Metcalfe, Chemosphere 73 (2008) 1741–1748.
[67] S. Contreras, M. Rodriguez, F. Al Momani, C. Sans, S. Esplugas, Water Res. 37 (2003) 3164–3171.

Update

Applied Catalysis B: Environmental
Volume 189, Issue , 15 July 2016, Page 283

DOI: https://doi.org/10.1016/j.apcatb.2016.02.027

Applied Catalysis B: Environmental 189 (2016) 283

Contents lists available at ScienceDirect

Applied Catalysis B: Environmental

journal homepage: www.elsevier.com/locate/apcatb

Corrigendum

Corrigendum to "Degradation of pharmaceuticals in wastewater using immobilized TiO_2 photocatalysis under simulated solar irradiation" [Appl. Catal. B: Environ. 182 (2016) 132–141]

Yujie He*, Nora B. Sutton, Huub H.M. Rijnaarts, Alette A.M. Langenhoff

Department of Environmental Technology, Wageningen University, P.O. Box 17, 6700 EV Wageningen, The Netherlands

The authors regret to inform that the initial name of one co-author is incorrect:
Huub H.H. Rijnaarts should be changed to Huub H.M. Rijnaarts.
Author would like to apologize for the inconvenience caused.

DOI of original article: http://dx.doi.org/10.1016/j.apcatb.2015.09.015.
* Corresponding author.
E-mail address: yujie.he@wur.nl (Y. He).

http://dx.doi.org/10.1016/j.apcatb.2016.02.027